RNA-sequencing analysis of aberrantly expressed long non-coding RNAs and mRNAs in a mouse model of ventilator-induced lung injury

BO XU[1,2], YIZHOU WANG[3], XIUJUAN LI[1], YANFEI MAO[2] and XIAOMING DENG[1]

[1]Department of Anesthesiology and Intensive Care, Changhai Hospital, Second Military Medical University, Shanghai 200433; [2]Department of Anesthesiology and SICU, Xinhua Hospital, School of Medicine, Shanghai Jiaotong University, Shanghai 200092; [3]Department of Hepatic Surgery IV, Eastern Hepatobiliary Surgery Hospital, Second Military Medical University, Shanghai 200438, P.R. China

Received November 7, 2017; Accepted March 22, 2018

DOI: 10.3892/mmr.2018.9034

Abstract. Long non-coding RNAs (lncRNAs) are closely associated with the regulation of various biological processes and are involved in the pathogenesis of numerous diseases. However, to the best of our knowledge, the role of lncRNAs in ventilator-induced lung injury (VILI) has yet to be evaluated. In the present study, high-throughput sequencing was applied to investigate differentially expressed lncRNAs and mRNAs (fold change >2; false discovery rate <0.05). Bioinformatics analysis was employed to predict the functions of differentially expressed lncRNAs. A total of 104 lncRNAs (74 upregulated and 30 downregulated) and 809 mRNAs (521 upregulated and 288 downregulated) were differentially expressed in lung tissues from the VILI group. Gene ontology analysis demonstrated that the differentially expressed lncRNAs and mRNAs were mainly associated with biological functions, including apoptosis, angiogenesis, neutrophil chemotaxis and skeletal muscle cell differentiation. The top four enriched pathways were the tumor necrosis factor (TNF) signaling pathway, P53 signaling pathway, neuroactive ligand-receptor interaction and the forkhead box O signaling pathway. Several lncRNAs were predicted to serve a vital role in VILI. Subsequently, three lncRNAs [mitogen-activated protein kinase kinase 3, opposite strand (Map2k3os), dynamin 3, opposite strand and abhydrolase domain containing 11, opposite strand] and three mRNAs (growth arrest and DNA damage-inducible α, claudin 4 and thromboxane A2 receptor) were measured by reverse transcription-quantitative polymerase chain reaction, in order to confirm the veracity of RNA-sequencing analysis. In addition, Map2k3os small interfering RNA transfection inhibited the expression of stretch-induced cytokines [TNF-α, interleukin (IL)-1β and IL-6] in MLE12 cells. In conclusion, the results of the present study provided a profile of differentially expressed lncRNAs in VILI. Several important lncRNAs may be involved in the pathological process of VILI, which may be useful to guide further investigation into the pathogenesis for this disease.

Correspondence to: Professor Xiaoming Deng, Department of Anesthesiology and Intensive Care, Changhai Hospital, Second Military Medical University, 168 Changhai Road, Shanghai 200433, P.R. China
E-mail: deng_x@yahoo.com

Professor Yanfei Mao, Department of Anesthesiology and SICU, Xinhua Hospital, School of Medicine, Shanghai Jiaotong University, 1665 Kongjiang Road, Shanghai 200092, P.R. China
E-mail: maoyanfei@xinhuamed.com.cn

Key words: long non-coding RNA, RNA-sequencing analysis, ventilator-induced lung injury, mouse

Introduction

Mechanical ventilation (MV) is an irreplaceable therapy for patients in intensive care units and emergency departments. Although the techniques for MV have significantly improved in the past 20 years (1), the risk of aggravating lung injury in patients with acute respiratory distress syndrome (ARDS) (2), and damaging healthy lung tissue, remains (3,4). Lung injury caused by MV is also known as ventilator-induced lung injury (VILI), and is characterized by tissue disruption, lung edema and pulmonary inflammation (5-7). A recent study from the ARDS Network indicated that VILI may increase the mortality of critically ill patients by ~10% (8). However, in addition to the protective pulmonary ventilation strategy, there are few specific treatments for VILI, as the potential mechanism remains poorly understood. Therefore, it is imperative to identify the pathogenesis of VILI to provide an experimental foundation for clinical treatment.

In the transcriptome, numerous protein-coding mRNAs, as well as non-protein coding transcripts, are closely associated with the pathogenesis of several diseases. Long non-coding RNAs (lncRNAs) are defined as non-protein coding transcripts >200 nucleotides long (9). In recent years, a growing body of evidence has indicated that lncRNAs are involved in various important biological processes, including proliferation (10), apoptosis (11), brain development (12,13),

inflammation (14,15) and immunoregulation (16,17), leading to numerous diseases (18-20); lncRNAs may therefore provide alternative targets for the treatment of these diseases (19,21).

Although the crucial roles of lncRNAs have been investigated in numerous diseases, to the best of the authors' knowledge, no study has been conducted to investigate the profile and function of lncRNAs in VILI. In the present study, differentially expressed lncRNAs and mRNAs were investigated by high-throughput sequencing, and bioinformatics analysis was employed to predict their functions in VILI.

Materials and methods

Animals. Experiments were performed on 16 male ICR mice (age, 7-9 weeks, 25-30 g; Shanghai SLAC Laboratory Animal Co., Shanghai, China). Mice were housed in a temperature-controlled room (22±2˚C) under a 12-h light/dark cycle, and were provided *ad libitum* access to food and water. The humidity was maintained at 50-60%. All experimental protocols and animal handling procedures were approved by the Ethics Committee on Experimental Animals of Shanghai Jiaotong University School of Medicine (Shanghai, China). Mice were divided into two groups: Sham-operated group and VILI group (n=8/group). A total of eight pairs of right lungs were used for RNA-sequencing (RNA-Seq) analysis, whereas eight pairs of left lungs were used for reverse transcription-quantitative polymerase chain reaction (RT-qPCR).

Establishment of a VILI mouse model. Following anesthesia with 100 mg/kg ketamine and 8 mg/kg xylazine (intraperitoneal), mice were fixed in a supine position, endotracheal intubation was performed and the tube was connected to a rodent ventilator (Inspira; Harvard Apparatus Ltd., Holliston, MA, USA). Ventilation was performed at a tidal volume of 30 ml/kg and a respiratory rate of 70 breaths/min for 4 h as previously described (22,23). Mice in the sham group underwent intubation but were allowed to breathe freely. Gas with fraction of inspired oxygen at 21% was used, and the inspiratory/expiratory ratio was 2:1. At the end of the experiment, animals were sacrificed by anesthetic overdose and the lung tissues were harvested for further investigation.

RNA-Seq analysis. Total RNA was extracted from lung tissues in the VILI and sham groups with TRIzol® (Invitrogen; Thermo Fisher Scientific, Inc., Waltham, MA, USA), according to the manufacturer's protocol. RNA concentration was determined using NanoDrop 2000 (NanoDrop; Thermo Fisher Scientific, Inc., Wilmington, DE, USA), and RNA quality was evaluated with Bioanalyzer 2200 (Agilent Technologies, Inc., Santa Clara, CA, USA) and by 1% agarose gel electrophoresis. RNA with RNA integrity number >8.0 was used to construct a cDNA library. A total of five pair of lungs met the criterion and were used for RNA-Seq analysis.

The cDNA libraries were subsequently constructed with Ion Total RNA-Seq kit version 2.0 (Thermo Fisher Scientific, Inc.). Subsequently, proton sequencing was performed using the cDNA libraries and Ion PI Sequencing 200 kit version 2.0 (Thermo Fisher Scientific, Inc.), according to the manufacturer's protocol. Briefly, samples were mixed and processed on the Ion OneTouch 2 System (Thermo Fisher Scientific, Inc.). Subsequently, they were enriched on the OneTouch 2 ES station for the preparation of template-positive Ion PI Ion Sphere Particles. Finally, the mixed samples were loaded onto 1 P1v2 Proton Chip (Thermo Fisher Scientific, Inc.) for sequencing. Data analysis was performed by NovelBio Bio-Pharm Technology Co., Ltd. (Shanghai, China).

RNA-seq mapping and identification of differentially expressed genes. The Mapsplice v2.2.0 program was used for RNA-seq data mapping (24). Per kilobase per million was used to measure the expression level of each gene (25). The expression of different genes between two groups was evaluated with the EB-Seq (26) algorithm. When the absolute fold change (FC) was >2 and the false discovery rate (FDR) was <0.05, the gene was defined as differentially expressed (26).

Gene ontology (GO) and pathway analysis. GO analysis was performed to analyze the biological functions of differentially expressed genes (27). GO annotations were obtained from gene in NCBI (https://www.ncbi.nlm.nih.gov/gene/) and the Gene Ontology (http://www.geneontoloy.org/). Kyoto Encyclopedia of Genes and Genomics (KEGG) database (http://www.genome.jp.kegg/) was employed to analyze the pathways associated with these differentially expressed genes (28). In addition, differentially expressed genes enriched in ≥2 biological pathways were selected to build the 'path-act network' a graphical representation of pathways of the interaction of these pathway terms using cytoscape 3.5.1 (29).

Gene co-expression network analysis. Gene co-expression network analysis, analyzed by R software 3.3.3, was employed to predict the key lncRNAs that function in the important biological processes and signal transduction pathways based on the correlation between differentially expressed lncRNAs and mRNAs (30). The significant correlation pairs (Pearson's correlation coefficient >0.95) were selected to build the network. The core regulatory genes were determined by k-core scoring in the network (31). The k-core indicates the hub or nodal status of a gene having interactions with other genes in the network. The higher the k-core score of a gene, the more central the gene location in the gene co-expression network.

RT-qPCR analysis. To confirm the veracity of RNA-Seq analysis, the expression of three lncRNAs and three mRNAs was measured by RT-qPCR using the SYBR-Green method (FastStart Universal SYBR Master; Roche Diagnostics, Basel, Switzerland) and a MiniOpticon real-time PCR detection system (Bio-Rad Laboratories, Inc., Hercules, CA, USA). Total RNA was extracted from lung tissues using TRIzol® reagent (Invitrogen; Thermo Fisher Scientific, Inc.) and cDNA was synthesized (RevertAid First Strand cDNA Synthesis kit; Thermo Fisher Scientific, Inc.) with the reaction conditions: 25˚C 10 min, 42˚C 1 h, 72˚C 10 min and 4˚C hold. All of the primers (Table I) used for RT-qPCR were designed and synthesized by Sangon Biotech Co., Ltd. (Shanghai, China). PCR was performed under the following conditions: Predenaturation for 2 min at 95˚C with cycle, denaturation for 15 sec at 95˚C, annealing for 15 sec at 60˚C and extension for 1 min at 72˚C with 40 cycles from denaturation to extension. The expression of each gene was calculated using the $2^{-\Delta\Delta Cq}$ (32) method and

Table I. Primers used for the amplification of various genes (long non-coding RNAs and mRNAs) in mouse lung tissues.

Description	Sequence (5'-3')	Product size (bp)	Accession no.
Map2k3os, F	AGCAAAGCAACAGCCTCACT	1,267	NR_027800.1
Map2k3os, R	CACGGGCTCTCTGTGCTTAT		
Dnm3os, F	GCCTGGCTGGACAGAGTTGT	7,928	NR_002870.2
Dnm3os, R	TCAATGGCTGGTGGTCATTC		
Abhd11os, F	CAGTCACCAGGCCTTGACTC	519	NR_026688.1
Abhd11os, R	CGCTTCTTAGCAATGGCTTC		
Gadd45a, F	CTGCAGAGCAGAAGACCGAA	1,224	NM_007836.1
Gadd45a, R	GGGTCTACGTTGAGCAGCTT		
Cldn4, F	GGCGTCTATGGGACTACAGG	1,827	NM_009903.2
Cldn4, R	GAGCGCACAACTCAGGATG		
Tbxa2r, F	GCTCATCTACCTGCGTGTGG	1,809	NM_001277265.1
Tbxa2r, R	CAGCCTGGAGCTGTGAACTG		
β-actin, F	CTGTATGCCTCTGGTCGTAC	214	NM_007393.3
β-actin, R	TGATGTCACGCACGATTTCC		

Abhd11os, abhydrolase domain containing 11, opposite strand; Cldn4, claudin 4; Dnm3os, dynamin 3, opposite strand; F, forward; Gadd45a, growth arrest and DNA damage-inducible α; Map2k3os, mitogen-activated protein kinase kinase 3, opposite strand; R, reverse; Tbxa2r, thromboxane A2 receptor.

normalized to that of β-actin. The experiments were repeated twice.

Cell culture and treatment. To determine the function of differentially expressed lncRNAs, the effects of Map2k3os were measured on the release of inflammatory cytokines from alveolar epithelial cells induced by cyclic stretch. The MLE12 [Obio Technology (Shanghai) Corp., Ltd., Shanghai, China] murine lung epithelial cell line was cultured with Dulbecco's modified Eagle's medium (HyClone; GE Healthcare Life Sciences, Logan, UT, USA) supplemented with 10% fetal bovine serum (Gibco; Thermo Fisher Scientific, Inc.) at 37˚C in an atmosphere containing 5% CO_2 (33). Map2k3os small interfering RNA (siRNA) was synthesized by Shanghai GenePharma Co., Ltd. (Shanghai, China), as was the negative control siRNA. The sequence of mouse Map2k3os siRNA was: 5'-CCCAUGGGAAGCAAAGCAATT-3'. The sequence of negative control siRNA was: 5'-UUCUCCGAACGUGUC ACGUTT-3'. MLE-12 cells were seeded onto Collagen I-coated Bioflex 6-well culture plates (BFI products, Inc., Hollywood, FL, USA). When the cells reached 80% coverage of one well, they were transfected with siRNA (60 pmol/ml) using Xfect siRNA transfection reagents (Takara Bio, Inc., Otsu, Japan). Following transfection for 24 h, the medium was renewed and the cells were subjected to cyclic stretch (20% linear elongation, sinusoidal wave, 30 cycles/min) for 4 h, as previously described (34), using the Flexcell-FX-5,000 Tension system (Flexcell International Corporation, Burlington, NC, USA). Control cells were placed in the same culture plates and incubated next to the stretched cells at 37˚C in an atmosphere containing 5% CO_2. Following cyclic stretch, the cells were harvested to analyze the expression of interleukin (IL)-1β, IL-6 and tumor necrosis factor (TNF)-α by RT-qPCR conducted as previously described in the RT-qPCR subsection. The primer sequences (Sangon Biotech Co., Ltd.) were as follows: IL-1β forward, 5'-TCGCAGCAGCACATCAACAAGAG-3' and reverse, 5'-TGCTCATGTCCTCATCCTGGAAGG-3'; IL-6 forward, 5'-ACTTCCATCCAGTTGCCTTCTTGG-3' and reverse, 5'-TTAAGCCTCCGACTTGTGAAGTGG-3'; and TNF-α forward, 5'-GCGACGTGGAACTGGCAGAAG-3' and reverse, 5'-GCCACAAGCAGGAATGAGAAGAGG-3'.

ELISA. Following cyclic stretch, the conditioned medium was collected. IL-1β (cat. no. F10770), IL-6 (cat. no. F10830) and TNF-α (cat. no. F11630) concentrations were determined using ELISA kits (Shanghai Westang Biotechnology Co., Ltd., Shanghai, China) for mice, according to the manufacturer's protocols.

Statistical analysis. All data were analyzed with SPSS version 20.0 (IBM Corp., Armonk, NY, USA). Student's t-test was applied to identify the differently expressed lncRNAs and mRNAs following RNA-Seq and RT-qPCR. According to previous studies (35,36), Fisher's exact test and χ^2 test were used to examine the significance of GO category and pathway analysis. FDR was used to correct the multiple testing to minimize the error of P-value (37,38), and in RNA-Seq to identify the differentially expressed genes (FDR<0.05). One-way analysis of variance followed by Dunnett's test for multiple comparisons was use to compare the difference between multiple groups. P<0.05 was considered to indicate a statistically significant difference.

Results

Differentially expressed lncRNAs and mRNAs. LncRNA and mRNA expression between the VILI and sham groups was analyzed using the DE-Seq algorithm, and differentially expressed genes were identified. A total of 104 lncRNAs and 809 mRNAs were identified as differentially expressed between the groups by

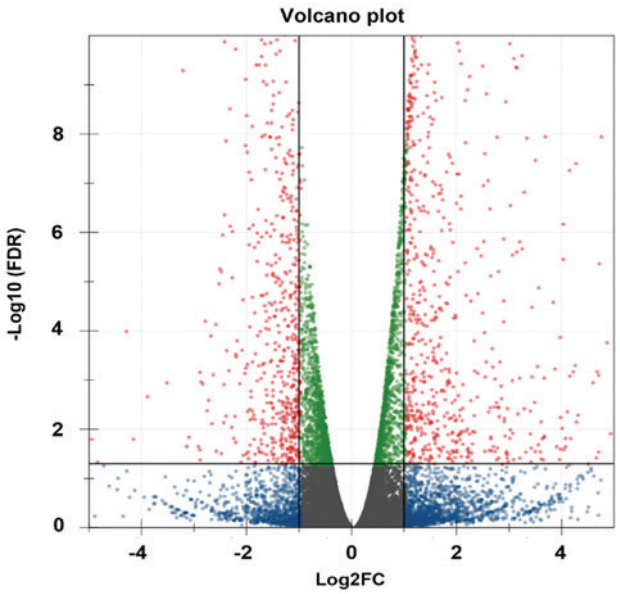

Figure 1. Differentially expressed genes between sham and ventilator-induced lung injury groups. The volcano plot includes all of the genes in the two groups. Differentially expressed genes are marked as red dots (FDR<0.05), other genes are marked as blue or green dots. Blue dots meant FDR≥0.05, green dots meant -2≤FC≤2. FC, fold change; FDR, false discovery rate.

high-throughput sequencing. Among the 104 lncRNAs, 74 were upregulated and 30 were downregulated. Of the 809 mRNAs, 521 were upregulated and 288 were downregulated. Volcano plot was used to identify differentially expressed genes (lncRNAs and mRNAs) between the two groups; when the expression was similar, the genes were marked blue, whereas the differentially expressed genes (FC>2 and FDR<0.05) were marked red (Fig. 1). The top 20 differentially expressed genes are presented in Table II (10 upregulated and 10 downregulated lncRNAs). To validate the results from RNA-Seq, the expression levels of three lncRNAs (Map2k3os, Dnm3os and Abhd11os) and three mRNAs (Gadd45a, Cldn4 and Tbxa2r) were detected by RT-qPCR. The results demonstrated that the change in the expression of these lncRNAs and mRNAs determined by RT-qPCR was similar to that from RNA-Seq (Fig. 2A and B).

GO analysis. GO analysis indicated that the differentially expressed mRNAs were associated with numerous important biological processes, cellular components and molecular functions. The present study indicated that 189 GO terms (147 upregulated and 42 downregulated) associated with biological processes were enriched (P<0.01, FDR<0.05). The primary upregulated GO categories were mainly involved in cell apoptosis, neutrophil chemotaxis, inflammatory response, cell proliferation and response to glucocorticoid (Fig. 3A), whereas the downregulated categories were mainly associated with the positive regulation of transcription (DNA-templated), cell-cell signaling, cellular response to interferon-γ, cell cycle and positive regulation of cytosolic calcium concentration (Fig. 3B).

Pathway enrichment analysis. The pathway enrichment analysis was employed to investigate the pathways associated with important differentially expressed genes. -Lg P-value was used to describe the significance level of pathway enrichment.

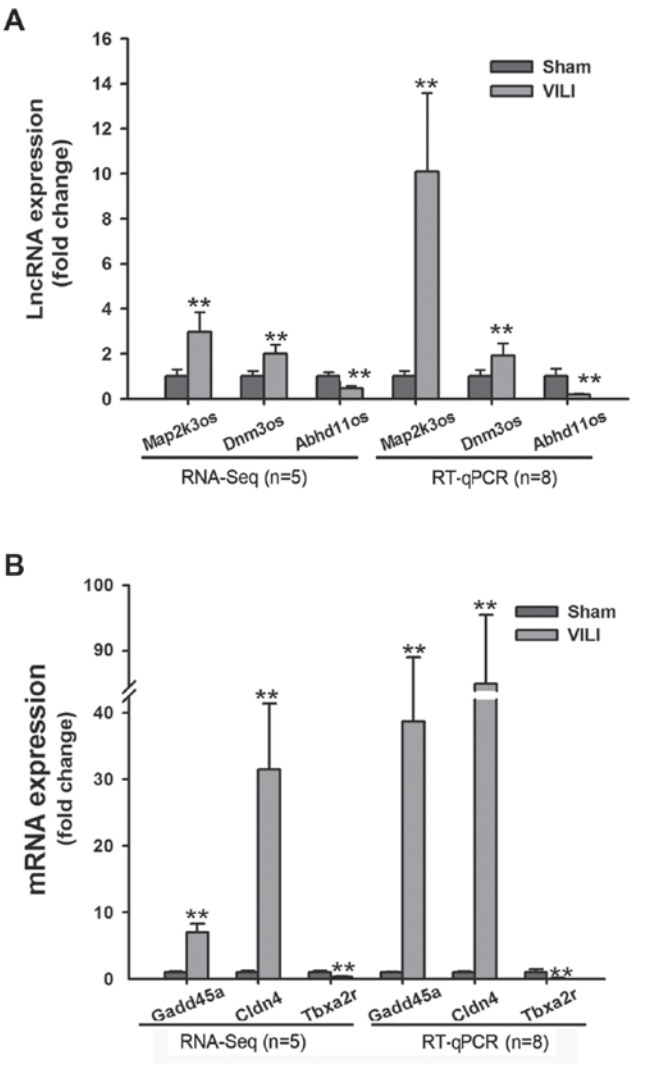

Figure 2. (A) Three lncRNAs (Map2k3os, Dnm3os and Abhd11os) identified by RNA-Seq were verified by RT-qPCR. **P<0.01 vs. the sham group. (B) Three mRNAs (Gadd45a, Cldn4 and Tbxa2r) identified by RNA-Seq were verified by RT-qPCR. **P<0.01 vs. the sham group. Abhd11os, abhydrolase domain containing 11, opposite strand; Cldn4, claudin 4; Dnm3os, dynamin 3, opposite strand; Gadd45a, growth arrest and DNA damage-inducible α; lncRNA, long non-coding RNA; Map2k3os, mitogen-activated protein kinase kinase 3, opposite strand; RNA-Seq, RNA-sequencing; RT-qPCR, reverse transcription-quantitative polymerase chain reaction; Tbxa2r, thromboxane A2 receptor.

There were 60 upregulated pathways and 21 downregulated pathways. The top 20 differentially expressed pathways with upregulated expression were mainly associated with the TNF, hypoxia-inducible factor (HIF)-1, p53 and Forkhead box O signaling pathways, and those with downregulated expression were associated with neuroactive ligand-receptor interaction, Hippo signaling pathway, phenylalanine metabolism and calcium signaling pathway (Fig. 4A). The differentially expressed genes in these pathways provide evidence for further investigations of the potential mechanisms underlying the pathogenesis of VILI. The interactions between these pathways are illustrated in Fig. 4B.

LncRNA-mRNA co-expression network. LncRNA-mRNA co-expression network was constructed based on the

Table II. Top 20 differentially expressed lncRNAs (10 upregulated and 10 downregulated lncRNAs) between ventilator-induced lung injury group and sham group.

AccID	FDR	Regulation	Location	Description
Gm4610	9.71×10^{-27}	Up	chr3	Predicted gene 4610
LOC102636324	1.55×10^{-16}	Up	chr13	Uncharacterized LOC102636324
Gm11827	2.74×10^{-15}	Up	chr4	Predicted gene 11827
LOC101056163	1.01×10^{-12}	Up	chr8	14-3-3 protein sigma-like
Gm5582	3.60×10^{-12}	Up	chr6	Predicted gene 5582
Serpina3h	5.07×10^{-12}	Up	chr12	Serpina3h protein
Krt8-ps	9.79×10^{-10}	Up	chr7	Keratin 8, pseudogene
Gm9523	4.19×10^{-9}	Up	chr5	Methionine adenosyltransferase II, alpha pseudogene
LOC102633421	9.00×10^{-9}	Up	chr11	14-3-3 protein sigma-like
Mir22hg	3.83×10^{-8}	Up	chr11	Mir22 host gene (non-protein coding)
Gm16119	3.98×10^{-8}	Down	chr2	Uridine-cytidine kinase 1-like 1, opposite strand
LOC102632993	6.82×10^{-8}	Down	chr7	Uncharacterized LOC102632993
LOC102635638	4.02×10^{-7}	Down	chr9	Uncharacterized LOC102635638
9630028I04Rik	8.16×10^{-7}	Down	chr17	RIKEN cDNA 9630028I04 gene
A330009N23Rik	4.05×10^{-6}	Down	chr15	RIKEN cDNA A330009N23 gene
AI197445	3.76×10^{-5}	Down	chr13	Expressed sequence AI197445
D930048N14Rik	1.05×10^{-4}	Down	chr11	Protein D930048N14Rik
Panct2	1.57×10^{-4}	Down	chr1	Pluripotency-associated noncoding transcript 2
5930430L01Rik	3.56×10^{-4}	Down	chr5	Katanin p60 ATPase-containing subunit A-like 1
2610507I01Rik	5.23×10^{-4}	Down	chr11	RIKEN cDNA 2610507I01 gene

FDR, false discovery rate.

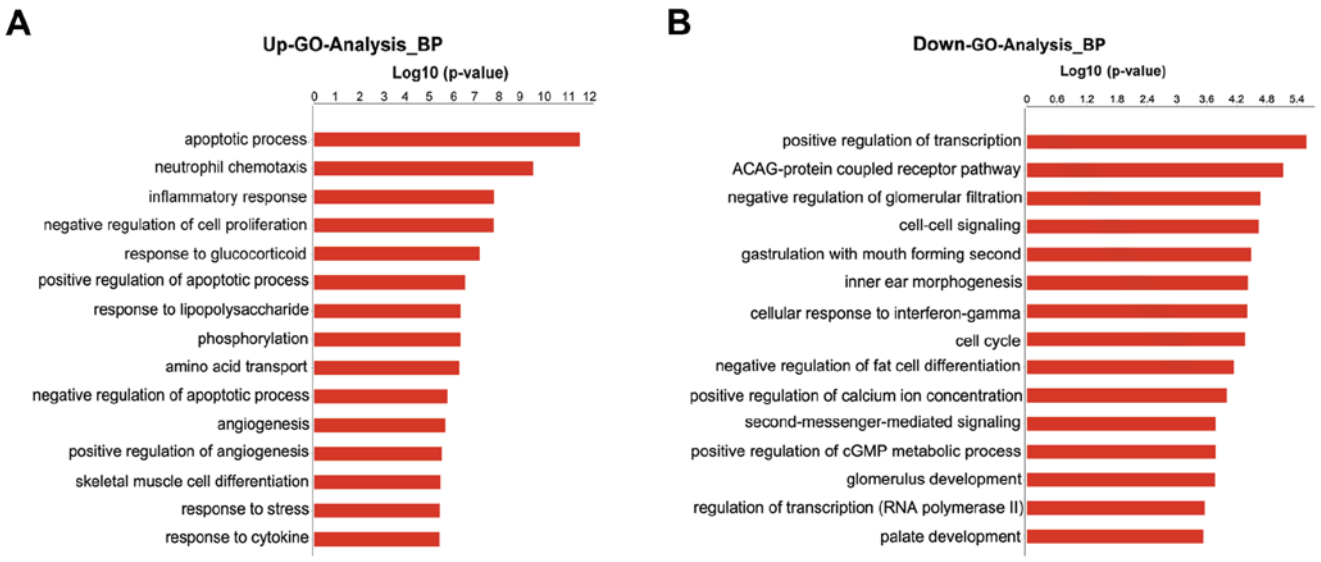

Figure 3. GO analysis based on differential genes between sham and ventilator-induced lung injury groups. (A) Top 15 GO categories for upregulated genes. (B) Top 15 GO categories for downregulated genes (FDR<0.05). FDR, false discovery rate; GO, gene ontology.

differentially expressed genes detected between the VILI and sham group lung tissues. There were 182 network nodes and 509 connections between genes in the VILI group. In this co-expression network, 272 pairs had positive association and 237 pairs exhibited negative association (Fig. 5). The properties of the constructed gene networks were determined by k-cores and the degree of differences. In the co-expression network, lncRNAs with differential degree ≥10 and k-core ≥8 included RIKEN cDNA 4933407K13 gene (4933407K13Rik), RIKEN cDNA E230013L22 gene (E230013L22Rik), RIKEN cDNA 3010003L21 gene (3010003L21Rik), RIKEN cDNA A330009N23 gene (A330009N23Rik), protein

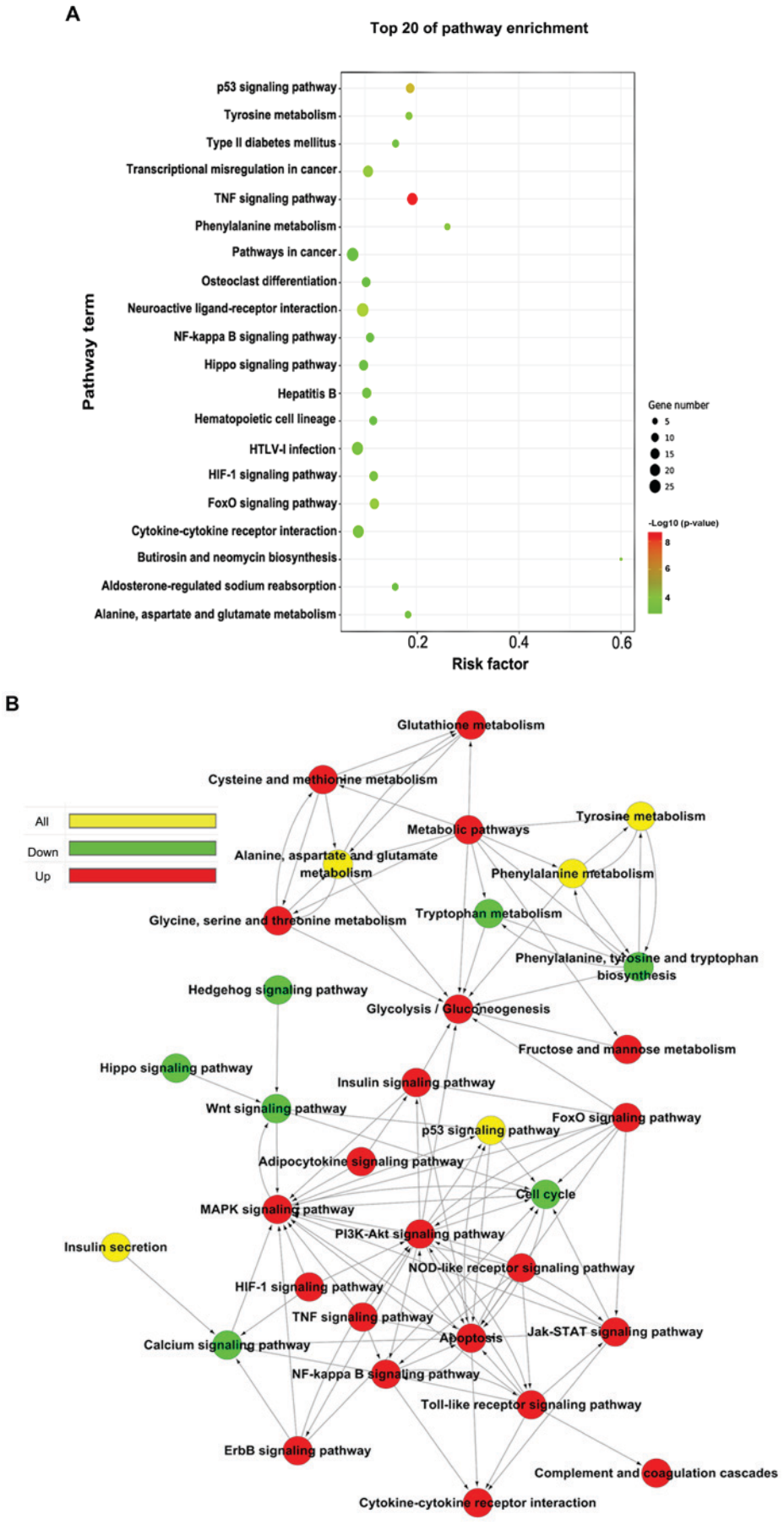

Figure 4. Pathway analysis of differentially expressed genes based on the KEGG database. (A) Top 20 signaling pathways, as determined by KEGG. (B) Interactions between the differential signaling pathways (path-act network, a graphical representation of pathways of the interaction of these pathway terms using cytoscape 3.5.1). Red dots represent upregulated pathways, green dots represent downregulated pathways and yellow dots represent bidirectional pathways. KEGG, Kyoto Encyclopedia of Genes and Genomics.

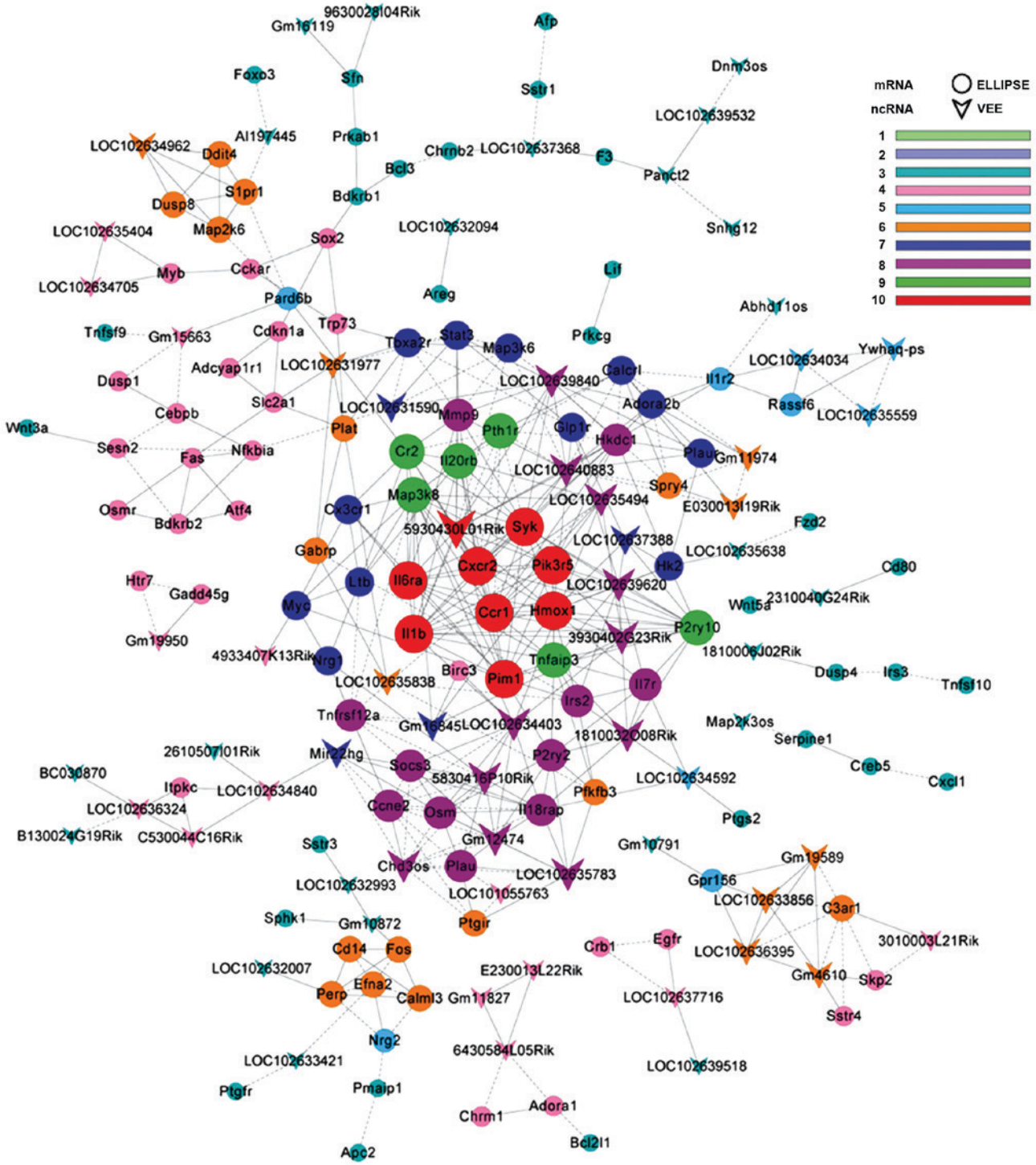

Figure 5. Co-expression network of differential genes in the ventilator-induced lung injury group.

D930048N14Rik (D930048N14Rik), predicted gene 11827 (Gm11827) and predicted gene 10872 (Gm10872). The top 20 differentially expressed lncRNAs, as determined by the gene co-expression analysis, are presented in Table III. These differentially expressed lncRNAs may be responsible for the potential mechanism underlying VILI.

Effects of Map2k3os siRNA on inflammatory cytokine release from MLE12 cells. Compared with in the control cells, it was identified that Map2k3os siRNA decreased the expression of Map2k3os by 89%, as determined by RT-qPCR (Table IV). Cyclic stretch significantly increased the mRNA expression levels of TNF-α, IL-1β and IL-6 in MLE12 cells, and protein levels in the supernatants. Conversely, Map2k3os siRNA transfection inhibited the expression of these stretch-induced cytokines (Fig. 6). These results indicated the effects of Map2k3os on epithelial secretion of cytokines in cyclic stretch-induced VILI.

Discussion

In the present study, RNA-Seq analysis identified 104 lncRNAs and 809 mRNAs, which were differentially expressed in

Table III. Top 20 differentially expressed long non-coding RNAs in the gene co-expression network.

AccID	DifKcore	DifDegree	Description
D930048N14Rik	10	19	Protein D930048N14Rik
Gm10872	9	14	predicted gene 10872
E230013L22Rik	8	19	RIKEN cDNA E230013L22 gene
Gm11827	8	13	predicted gene 11827
4933407K13Rik	8	19	RIKEN cDNA 4933407K13 gene
3010003L21Rik	8	17	RIKEN cDNA 3010003L21 gene
A330009N23Rik	8	17	RIKEN cDNA A330009N23 gene
B130024G19Rik	7	14	Putative uncharacterized protein
Panct2	7	10	Pluripotency-associated noncoding transcript 2
Chd3os	4	4	Putative uncharacterized protein RNF21
AI197445	4	4	Expressed sequence AI197445
Ywhaq-ps	3	6	Tyrosine 3-monooxygenase/tryptophan 5-monooxygenase activation protein, theta polypeptide, pseudogene 1
9630028I04Rik	3	6	RIKEN cDNA 9630028I04 gene
LOC102635838	2	6	Uncharacterized LOC102635838
Snhg12	2	3	Small nucleolar RNA host gene 12
Map2k3os	2	6	Mitogen-activated protein kinase kinase 3, opposite strand
4930481A15Rik	2	2	MCG1045479, isoform CRA_b
1810006J02Rik	1	3	RIKEN cDNA 1810006J02 gene
LOC102632993	1	1	Uncharacterized LOC102632993
LOC102637368	1	1	Uncharacterized LOC102637368

DifDegree, differential degree; DifKcore, differential key core.

lung tissues between the VILI group and the sham group. Bioinformatics analysis predicted several lncRNAs that were likely to alter the transcription of related mRNAs, and thus participate in the development of VILI. To the best of the authors' knowledge, the present study is the first to analyze the function of lncRNAs in VILI using high-throughput sequencing and bioinformatics analysis.

At present, there have been few studies regarding the transcriptomics of VILI (39-41). These previous studies used microarray analysis, and to the best of the authors' knowledge, a previous study tested the lncRNAs. Ma *et al* (39) focused on early stress response genes in rodents (mouse and rat) following VILI, and identified 41 upregulated genes and 7 downregulated genes in the injured lungs. GO analysis revealed that these genes may be involved in cell cycle arrest, immune response, inflammatory response, blood coagulation, chemotaxis, apoptosis, cell-cell signaling and negative regulation of cell proliferation (39). Another study (40) only reported inflammasome-related gene expression, including IL-1α, caspase-activator domain-10, and IL-1 receptor-1 and -2. Furthermore, a previous study (41) used microarray analysis to identify the effects of non-muscle myosin light chain kinase isoform on VILI. This study also identified alterations in the expression of several genes in VILI, including thioredoxin domain-containing 9, C-X-C motif chemokine ligand 2 and MYB proto-oncogene, transcription factor. As in previous studies, all of the biological processes reported and the majority of genes identified were also observed in the present study. The difference in the differentially expressed genes among available studies is possibly ascribed to the difference in species (mouse and rat vs. mouse) and methodology (microarray vs. high-throughput sequencing). In the present study, not only mRNAs, but also lncRNAs, were analyzed in the lung tissues, and GO analysis, pathway enrichment analysis, and lncRNA-mRNA co-expression networks were employed to predict the function of lncRNAs. Therefore, the findings may provide evidence regarding the mechanism underlying VILI and aid the development of novel targets to treat VILI.

The onset of VILI is associated with several biological processes and signaling pathways. MV can damage the lungs by direct mechanical injury and indirectly via the induction of biotrauma. Several signaling pathways and mRNAs identified in the present study have been identified in previous

Table IV. Effects of siRNA on long non-coding RNA Map2k3os expression in MLE12 cells (n=4).

Group	Relative expression	Relative reduction (%)
Control siRNA	1±0.184	0
Map2k3os siRNA	0.106±0.042[a]	89

Map2k3os, mitogen-activated protein kinase kinase 3, opposite strand; siRNA, small interfering RNA. Data is presented as the mean ± standard error. [a]P<0.01 compared with control siRNA group.

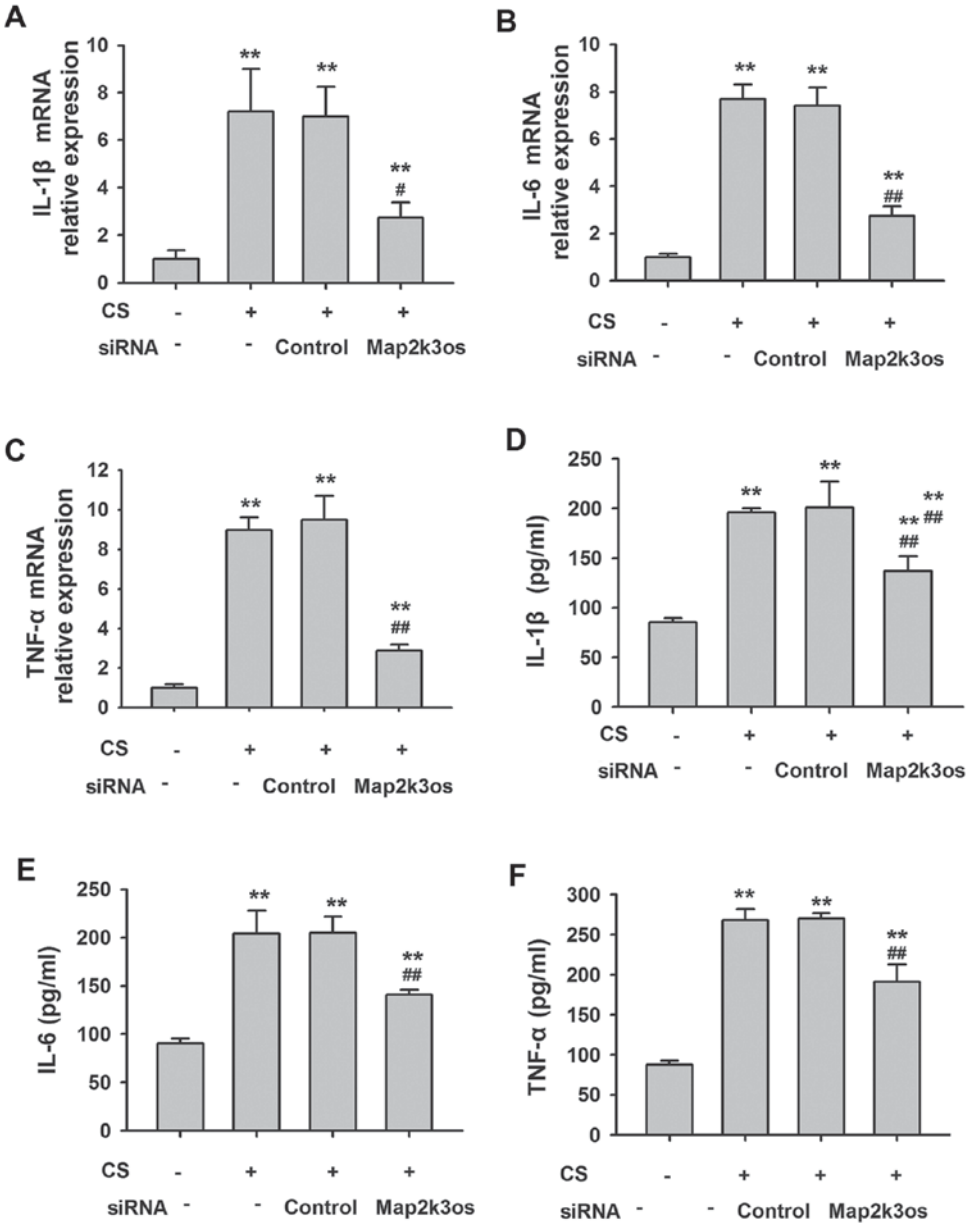

Figure 6. mRNA expression levels of (A) IL-1β, (B) IL-6 and (C) TNF-α in MLE12 cells, as determined by RT-qPCR. Protein level of (D) IL-1β, (E) IL-6 and (F) TNF-α in the culture medium, as determined by ELISA. (n=6). **P<0.01 compared with control group without cyclic stretch or siRNA. $^{\#\#}$P<0.01 compared with control siRNA group. CS, cyclic stretch; IL, interleukin; Map2k3os, mitogen-activated protein kinase kinase 3, opposite strand; RT-qPCR, reverse transcription-quantitative polymerase chain reaction; siRNA, small interfering RNA; TNF, tumor necrosis factor.

studies. Hyperinflation of mouse lungs *in vivo* and *in vitro* can induce the expression of nuclear factor (NF)-κB and IL-6 in alveolar macrophages and alveolar epithelial type II cells (42). In addition, chemokines [chemokine (C-X-C motif) ligand 1, cytokine-induced neutrophil chemoattractant-2α and macrophage inflammatory protein 2 (MIP-2)] and their receptors are activated during lung injury (43). The neutrophil elastase inhibitor sivelestat is able to inhibit neutrophil accumulation, and decrease the release of MIP-2, IL-6 and TNF-α in VILI mice (44). The present study also confirmed the important role of inflammatory response, neutrophil chemotaxis and the NF-κB signaling pathway. In addition, apoptosis was identified as the first key biological process in VILI by high-throughput sequencing. Previous studies also identified that pathological cyclic stretch could induce pulmonary epithelial apoptosis and barrier dysfunction in alveolar epithelial cells (45,46). Conversely, a previous study reported that ventilation at low tidal volumes results in a mild inflammatory response without increasing apoptosis, which is accompanied by accelerated alveolar epithelial cell proliferation (47). This differs from the results of the present study, which may be ascribed to the low tidal volume used in the previous study.

KEGG pathway analysis in the present study also demonstrated that several signaling pathways were associated with the pathogenesis of VILI. TNF is able to regulate pulmonary alveolar permeability, alveolar fluid clearance, adhesion molecule expression and leucocyte recruitment (48). TNF has been identified as a marker of early activation of inflammation and can be rapidly released in response to cyclic stretch (49,50). In

addition, HIF-1 can promote transcription of A2B adenosine receptor (A2BAR), whereas deletion of the A2BAR gene could reduce survival time and increase pulmonary albumin leakage following VILI (51,52). Furthermore, although the specific role of the P53 signaling pathway in VILI has not been reported, microarray assay has revealed it is involved in the pathogenesis of VILI (41). In the present study, a number of genes were differentially expressed between the sham group and the VILI group. Some genes have been verified by previous studies (49,53), whereas others may be novel targets with which to explore the mechanisms of VILI.

In the lncRNA-mRNA co-expression network, 4933407K13Rik, E230013L22Rik, 3010003L21Rik, A330009N23Rik, D930048N14Rik, Gm11827 and Gm10872 were most likely to be responsible for the potential mechanism underlying VILI. These lncRNAs may directly and indirectly regulate the transcription of related mRNAs, thus participating in the development of VILI. The top 20 differentially expressed lncRNAs are main target genes for future study. The present study confirmed that transfection with siRNA targeting Map2k3os (one of the top 20 lncRNAs) inhibited stretch-induced cytokine (TNF-α, IL-1β and IL-6) expression in MLE12 cells. However, further experiments are required to study the detailed function and mechanism of these lncRNAs in VILI. In addition, next-generation sequencing technology itself has certain limitations, including flux, which means the number of RNA samples that can be measured by a sequenator at the same time, is not high enough and the length of RNA reads remains relatively short (54), which may be improved with the development of improved technology.

In conclusion, the present study provided novel information regarding the lncRNAs, signaling pathways and the co-expression network involved in VILI. Numerous significant lncRNAs are likely to participate in the pathogenesis of VILI, which may be useful to guide further research into the mechanisms and targeted therapy for this disease.

Acknowledgements

The authors wish to thank Dr Yan Wang and Dr Chufan Xu (Department of Anesthesiology and SICU, Xinhua Hospital, Shanghai Jiaotong University, School of Medicine) for their technical assistance.

Funding

The present study was supported by grants from the National Natural Science Foundation of China (grant nos. 81100826, 81372100 and 81772108).

Availability of data and materials

The datasets used and/or analyzed during the current study are available from the corresponding author on reasonable request.

Authors' contributions

All authors participated in study design of the research question. BX contributed to model building, performing the ELISA and writing the manuscript. YW helped to perform RT-qPCR and analyze data. XL performed cell culture and statistics. YM and XD mainly designed the research and revised the manuscript.

Ethics approval and consent to participate

All experimental protocols and animal handling procedures were approved by the Ethics Committee on Experimental Animals of Shanghai Jiaotong University School of Medicine (Shanghai, China).

Consent for publication

Not applicable.

Competing interests

The authors declare that they have no competing interests.

References

1. Brower RG and Fessler HE: Mechanical ventilation in acute lung injury and acute respiratory distress syndrome. Clin Chest Med 21: 491-510, viii, 2000.
2. Belperio JA, Keane MP, Lynch JP III and Strieter RM: The role of cytokines during the pathogenesis of ventilator-associated and ventilator-induced lung injury. Semin Respir Crit Care Med 27: 350-364, 2006.
3. Neto AS, Simonis FD, Barbas CS, Biehl M, Determann RM, Elmer J, Friedman G, Gajic O, Goldstein JN, Linko R, *et al*: Lung-protective ventilation with low tidal volumes and the occurrence of pulmonary complications in patients without acute respiratory distress syndrome: A systematic review and individual patient data analysis. Crit Care Med 43: 2155-2163, 2015.
4. Serpa Neto A, Hemmes SN, Barbas CS, Beiderlinden M, Biehl M, Binnekade JM, Canet J, Fernandez-Bustamante A, Futier E, Gajic O, *et al*: Protective versus conventional ventilation for surgery: A systematic review and individual patient data meta-analysis. Anesthesiology 123: 66-78, 2015.
5. Choi WI, Quinn DA, Park KM, Moufarrej RK, Jafari B, Syrkina O, Bonventre JV and Hales CA: Systemic microvascular leak in an in vivo rat model of ventilator-induced lung injury. Am J Respir Crit Care Med 167: 1627-1632, 2003.
6. Slutsky AS and Ranieri VM: Ventilator-induced lung injury. N Engl J Med 369: 2126-2136, 2013.
7. Li Q, Ge YL, Li M, Fang XZ, Yuan YP, Liang L and Huang SQ: miR-127 contributes to ventilator-induced lung injury. Mol Med Rep 16: 4119-4126, 2017.
8. Brower RG, Lanken PN, MacIntyre N, Matthay MA, Morris A, Ancukiewicz M, Schoenfeld D and Thompson BT; National Heart, Lung, and Blood Institute ARDS Clinical Trials Network: Higher versus lower positive end-expiratory pressures in patients with the acute respiratory distress syndrome. N Engl J Med 351: 327-336, 2004.
9. Ponting CP, Oliver PL and Reik W: Evolution and functions of long noncoding RNAs. Cell 136: 629-641, 2009.
10. Su JC and Hu XF: Long non-coding RNA HOXA11-AS promotes cell proliferation and metastasis in human breast cancer. Mol Med Rep 16: 4887-4894, 2017.
11. Yang N, Chen J, Zhang H, Wang X, Yao H, Peng Y and Zhang W: LncRNA OIP5-AS1 loss-induced microRNA-410 accumulation regulates cell proliferation and apoptosis by targeting KLF10 via activating PTEN/PI3K/AKT pathway in multiple myeloma. Cell Death Dis 8: e2975, 2017.
12. Delás MJ and Hannon GJ: lncRNAs in development and disease: From functions to mechanisms. Open Biol 7: pii: 170121, 2017.
13. Ren C, Deng M, Fan Y, Yang H, Zhang G, Feng X, Li F, Wang D, Wang F and Zhang Y: Genome-wide analysis reveals extensive changes in LncRNAs during skeletal muscle development in Hu sheep. Genes (Basel) 8: pii: E191, 2017.

14. Zhang HJ, Wei QF, Wang SJ, Zhang HJ, Zhang XY, Geng Q, Cui YH and Wang XH: LncRNA HOTAIR alleviates rheumatoid arthritis by targeting miR-138 and inactivating NF-κB pathway. Int Immunopharmacol 50: 283-290, 2017.
15. Yi H, Peng R, Zhang LY, Sun Y, Peng HM, Liu HD, Yu LJ, Li AL, Zhang YJ, Jiang WH and Zhang Z: LincRNA-Gm4419 knockdown ameliorates NF-κB/NLRP3 inflammasome-mediated inflammation in diabetic nephropathy. Cell Death Dis 8: e2583, 2017.
16. Jiang R, Tang J, Chen Y, Deng L, Ji J, Xie Y, Wang K, Jia W, Chu WM and Sun B: The long noncoding RNA lnc-EGFR stimulates T-regulatory cells differentiation thus promoting hepatocellular carcinoma immune evasion. Nat Commun 8: 15129, 2017.
17. Mumtaz PT, Bhat SA, Ahmad SM, Dar MA, Ahmed R, Urwat U, Ayaz A, Shrivastava D, Shah RA and Ganai NA: LncRNAs and immunity: Watchdogs for host pathogen interactions. Biol Proced Online 19: 3, 2017.
18. Misawa A, Takayama KI and Inoue S: Long non-coding RNAs and prostate cancer. Cancer Sci 108: 2107-2114, 2017.
19. Haemmig S, Simion V, Yang D, Deng Y and Feinberg MW: Long noncoding RNAs in cardiovascular disease, diagnosis, and therapy. Curr Opin Cardiol 32: 776-783, 2017.
20. Zhuang YT, Xu DY, Wang GY, Sun JL, Huang Y and Wang SZ: IL-6 induced lncRNA MALAT1 enhances TNF-α expression in LPS-induced septic cardiomyocytes via activation of SAA3. Eur Rev Med Pharmacol Sci 21: 302-309, 2017.
21. Wahlestedt C: Targeting long non-coding RNA to therapeutically upregulate gene expression. Nat Rev Drug Discov 12: 433-446, 2013.
22. Li H, Su X, Yan X, Wasserloos K, Chao W, Kaynar AM, Liu ZQ, Leikauf GD, Pitt BR and Zhang LM: Toll-like receptor 4-myeloid differentiation factor 88 signaling contributes to ventilator-induced lung injury in mice. Anesthesiology 113: 619-629, 2010.
23. Li LF, Yang CT, Huang CC, Liu YY, Kao KC and Lin HC: Low-molecular-weight heparin reduces hyperoxia-augmented ventilator-induced lung injury via serine/threonine kinase-protein kinase B. Respir Res 12: 90, 2011.
24. Wang K, Singh D, Zeng Z, Coleman SJ, Huang Y, Savich GL, He X, Mieczkowski P, Grimm SA, Perou CM, *et al*: MapSplice: Accurate mapping of RNA-seq reads for splice junction discovery. Nucleic Acids Res 38: e178, 2010.
25. Mortazavi A, Williams BA, McCue K, Schaeffer L and Wold B: Mapping and quantifying mammalian transcriptomes by RNA-Seq. Nat Methods 5: 621-628, 2008.
26. Anders S and Huber W: Differential expression analysis for sequence count data. Genome Biol 11: R106, 2010.
27. Ashburner M, Ball CA, Blake JA, Botstein D, Butler H, Cherry JM, Davis AP, Dolinski K, Dwight SS, Eppig JT, *et al*: Gene ontology: Tool for the unification of biology. The Gene Ontology Consortium. Nat Genet 25: 25-29, 2000.
28. Kanehisa M, Goto S, Kawashima S, Okuno Y and Hattori M: The KEGG resource for deciphering the genome. Nucleic Acids Res 32 (Database Issue): D277-D280, 2004.
29. Shannon P, Markiel A, Ozier O, Baliga NS, Wang GT, Ramage D, Amin N, Schwikowski B and Ideker T: Cytoscape: A software environment for integrated models of biomolecular interaction networks. Genome Res 13: 2498-2504, 2003.
30. Pujana MA, Han JD, Starita LM, Stevens KN, Tewari M, Ahn JS, Rennert G, Moreno V, Kirchhoff T, Gold B, *et al*: Network modeling links breast cancer susceptibility and centrosome dysfunction. Nat Genet 39: 1338-1349, 2007.
31. Ravasz E, Somera AL, Mongru DA, Oltvai ZN and Barabási AL: Hierarchical organization of modularity in metabolic networks. Science 297: 1551-1555, 2002.
32. Livak KJ and Schmittgen TD: Analysis of relative gene expression data using real-time quantitative PCR and the 2(-Delta Delta C(T)) method. Methods 25: 402-408, 2001.
33. Sun D, Wang J, Yang N and Ma H: Matrine suppresses airway inflammation by downregulating SOCS3 expression via inhibition of NF-κB signaling in airway epithelial cells and asthmatic mice. Biochem Biophys Res Commun 477: 83-90, 2016.
34. Wang Y, Xu CF, Liu YJ, Mao YF, Lv Z, Li SY, Zhu XY and Jiang L: Salidroside attenuates ventilation induced lung injury via SIRT1-dependent inhibition of NLRP3 inflammasome. Cell Physiol Biochem 42: 34-43, 2017.
35. Wang W, Meng M, Zhang Y, Wei C, Xie Y, Jiang L, Wang C, Yang F, Tang W, Jin X, *et al*: Global transcriptome-wide analysis of CIK cells identify distinct roles of IL-2 and IL-15 in acquisition of cytotoxic capacity against tumor. BMC Med Genomics 7: 49, 2014.
36. Lin ZW, Gu J, Liu RH, Liu XM, Xu FK, Zhao GY, Lu CL and Ge D: Genome-wide screening and co-expression network analysis identify recurrence-specific biomarkers of esophageal squamous cell carcinoma. Tumour Biol 35: 10959-10968, 2014.
37. Benjamini Y and Hochberg Y: Controlling the false discovery rate: A practical and powerful approach to multiple testing. J R Stat Soc Series B 57: pp289-300, 1995.
38. Pawitan Y, Michiels S, Koscielny S, Gusnanto A and Ploner A: False discovery rate, sensitivity and sample size for microarray studies. Bioinformatics 21: 3017-3024, 2005.
39. Ma SF, Grigoryev DN, Taylor AD, Nonas S, Sammani S, Ye SQ and Garcia JG: Bioinformatic identification of novel early stress response genes in rodent models of lung injury. Am J Physiol Lung Cell Mol Physiol 289: L468-L477, 2005.
40. Dolinay T, Kim YS, Howrylak J, Hunninghake GM, An CH, Fredenburgh L, Massaro AF, Rogers A, Gazourian L, Nakahira K, *et al*: Inflammasome-regulated cytokines are critical mediators of acute lung injury. Am J Respir Crit Care Med 185: 1225-1234, 2012.
41. Mirzapoiazova T, Moitra J, Moreno-Vinasco L, Sammani S, Turner JR, Chiang ET, Evenoski C, Wang T, Singleton PA, Huang Y, *et al*: Non-muscle myosin light chain kinase isoform is a viable molecular target in acute inflammatory lung injury. Am J Respir Cell Mol Biol 44: 40-52, 2011.
42. Uhlig U, Fehrenbach H, Lachmann RA, Goldmann T, Lachmann B, Vollmer E and Uhlig S: Phosphoinositide 3-OH kinase inhibition prevents ventilation-induced lung cell activation. Am J Respir Crit Care Med 169: 201-208, 2004.
43. Vanderbilt JN, Mager EM, Allen L, Sawa T, Wiener-Kronish J, Gonzalez R and Dobbs LG: CXC chemokines and their receptors are expressed in type II cells and upregulated following lung injury. Am J Respir Cell Mol Biol 29: 661-668, 2003.
44. Sakashita A, Nishimura Y, Nishiuma T, Takenaka K, Kobayashi K, Kotani Y and Yokoyama M: Neutrophil elastase inhibitor (sivelestat) attenuates subsequent ventilator-induced lung injury in mice. Eur J Pharmacol 571: 62-71, 2007.
45. Hammerschmidt S, Kuhn H, Grasenack T, Gessner C and Wirtz H: Apoptosis and necrosis induced by cyclic mechanical stretching in alveolar type II cells. Am J Respir Cell Mol Biol 30: 396-402, 2004.
46. Gao J, Huang T, Zhou LJ, Ge YL, Lin SY and Dai Y: Preconditioning effects of physiological cyclic stretch on pathologically mechanical stretch-induced alveolar epithelial cell apoptosis and barrier dysfunction. Biochem Biophys Res Commun 448: 342-348, 2014.
47. Chess PR, Benson RP, Maniscalco WM, Wright TW, O'Reilly MA and Johnston CJ: Murine mechanical ventilation stimulates alveolar epithelial cell proliferation. Exp Lung Res 36: 331-341, 2010.
48. Mukhopadhyay S, Hoidal JR and Mukherjee TK: Role of TNFalpha in pulmonary pathophysiology. Respir Res 7: 125, 2006.
49. Wilson MR and Takata M: Inflammatory mechanisms of ventilator-induced lung injury: A time to stop and think? Anaesthesia 68: 175-178, 2013.
50. Wilson MR, Wakabayashi K, Bertok S, Oakley CM, Patel BV, O'Dea KP, Cordy JC, Morley PJ, Bayliffe AI and Takata M: Inhibition of TNF receptor p55 by a domain antibody attenuates the initial phase of acid-induced lung injury in mice. Front Immunol 8: 128, 2017.
51. Eckle T, Kewley EM, Brodsky KS, Tak E, Bonney S, Gobel M, Anderson D, Glover LE, Riegel AK, Colgan SP and Eltzschig HK: Identification of hypoxia-inducible factor HIF-1A as transcriptional regulator of the A2B adenosine receptor during acute lung injury. J Immunol 192: 1249-1256, 2014.
52. Eckle T, Grenz A, Laucher S and Eltzschig HK: A2B adenosine receptor signaling attenuates acute lung injury by enhancing alveolar fluid clearance in mice. J Clin Invest 118: 3301-3315, 2008.
53. Wang T, Gross C, Desai AA, Zemskov E, Wu X, Garcia AN, Jacobson JR, Yuan JX, Garcia JG and Black SM: Endothelial cell signaling and ventilator-induced lung injury: Molecular mechanisms, genomic analyses, and therapeutic targets. Am J Physiol Lung Cell Mol Physiol 312: L452-L476, 2017.
54. Hert DG, Fredlake CP and Barron AE: Advantages and limitations of next-generation sequencing technologies: A comparison of electrophoresis and non-electrophoresis methods. Electrophoresis 29: 4618-4626, 2008.